




A new fossil salamander (Caudata, Proteidae) from the Upper Cretaceous (Maastrichtian) Hell Creek Formation, Montana, U.S.A.

David G. Demar Jr.


To cite this article: David G. Demar Jr. (2013) A new fossil salamander (Caudata, Proteidae) from the Upper Cretaceous (Maastrichtian) Hell Creek Formation, Montana, U.S.A., *Journal of Vertebrate Paleontology*, 33:3, 588-598, DOI: [10.1080/02724634.2013.734887](https://doi.org/10.1080/02724634.2013.734887)

To link to this article: <http://dx.doi.org/10.1080/02724634.2013.734887>

 View supplementary material 

 Published online: 07 May 2013.

 Submit your article to this journal 

 Article views: 225

 View related articles 

A NEW FOSSIL SALAMANDER (CAUDATA, PROTEIDAE) FROM THE UPPER CRETACEOUS (MAASTRICHTIAN) HELL CREEK FORMATION, MONTANA, U.S.A.

DAVID G. DEMAR, JR.

Department of Biology, University of Washington, Seattle, Washington 98195, U.S.A., ddemar@u.washington.edu

ABSTRACT—North American Late Cretaceous salamanders are principally known by isolated atlantes and trunk vertebrae. Here I describe a new genus and species of fossil salamander, *Paranecturus garbanii*, gen. et sp. nov., based on these elements from the lower portions of the Hell Creek Formation (Maastrichtian), Garfield County, northeastern Montana, U.S.A. It is diagnosed by a unique combination of character states that include the presence of an alar-like process of the atlas and a groove on the posterior face of the neural arch and solid dorsal rib-bearers of the trunk vertebrae. My phylogenetic analysis of 13 caudate taxa and 23 atlantal and trunk vertebral characters recovered *P. garbanii* as a member of the Proteidae. *P. garbanii* represents the oldest fossil record of the Proteidae and demonstrates that this lineage was present before the Cretaceous–Paleogene mass extinction event.

SUPPLEMENTAL DATA—Supplemental materials are available for this article for free at www.tandfonline.com/UJVP

INTRODUCTION

Fossil salamanders (Caudata) are common components of latest Cretaceous vertebrate microfossil assemblages of the Western Interior of North America (e.g., Estes, 1964, 1981; Gardner, 2000; Holman, 2006; Wilson et al., in press). Three currently recognized clades are represented: Batrachosauroididae, Scapherpetontidae, and Sirenidae (Estes, 1981; Gardner, 2000, 2005; Holman, 2006). The Amphiumidae may also have had a latest Cretaceous presence (Estes, 1969); but see Gardner (2003a), DeMar (2011), and Wilson et al. (in press). The Proteidae are unequivocally known from the late Paleocene of southwestern Saskatchewan, Canada (*Necturus krausei*; Naylor, 1978a), whereas reports of Cretaceous and earlier occurrences of the family are unsubstantiated (Estes, 1981).

Caudates are well represented in the Upper Cretaceous (Maastrichtian) Hell Creek Formation of Montana (e.g., Estes and Berberian, 1970; Bryant, 1989; Gardner, 2000) and recent work in these deposits has recognized a total of nine species (Wilson et al., in press). Here I describe a new genus and species of caudate from Garfield County, northeastern Montana, U.S.A. (Fig. 1). *Paranecturus garbanii*, gen. et sp. nov., is based on isolated atlantes and trunk vertebrae from six distinct stratigraphic horizons in the lower three-fourths of the Hell Creek Formation. In addition to the description, I assessed the phylogenetic relationships of *P. garbanii* through a cladistic analysis of 13 caudate taxa and 23 vertebral characters. I find *P. garbanii* as the earliest member of Proteidae.

Institutional Abbreviations—**DMNH**, Denver Museum of Nature and Science (formerly the Denver Museum of Natural History), Denver, Colorado, U.S.A.; **MOR**, Museum of the Rockies, Bozeman, Montana, U.S.A.; **UALVP**, University of Alberta Laboratory for Vertebrate Paleontology, Edmonton, Alberta, Canada; **UCMP**, University of California Museum of Paleontology, Berkeley, California, U.S.A.; **UWBM**, University of Washington Burke Museum of Natural History and Culture, Seattle, Washington, U.S.A.

Anatomical Abbreviations—**aco**, anterior cotyle; **alp**, alar-like process; **bpr**, bony protuberance; **cc**, calcified cartilage; **dor**, dor-

sal ridge; **lf**, lateral fossa; **na**, neural arch; **nc**, neural canal; **npt**, notochordal pit; **nsp**, neural spine; **opr**, odontoid process; **opr(b)**, broken odontoid process; **pco**, posterior cotyle; **pnag**, groove on posterior face of neural arch; **popr**, postzygapophyseal process; **spfo**, spinal foramen; **sufo**, subcentral foramen; **ver**, ventral ridge; **vlf**, anterior ventrolateral foramen; **vlr**, ventrolateral ridge.

Other Abbreviation—**NALMA**, North American Land-Mammal ‘Age.’

MATERIALS AND METHODS

Osteological terms primarily come from Gardner (2003a). Measurements were made using a microscope with an ocular micrometer and from images measured via ImageJ 1.44p (Abramoff et al., 2004). Published descriptions and figures (Estes, 1964, 1965, 1975, 1981; Estes and Darevsky, 1977; Naylor, 1978a, 1978b, 1983; Naylor and Krause, 1981; Gardner, 2000, 2012) and direct observation of specimens of most taxa facilitated taxonomic comparisons and scoring for cladistic analysis. Observations of the skeletal anatomy of *Necturus* were based on *N. maculosus*. The stratigraphic positions of fossil localities are relative to the Hell Creek–Tullock formational contact in Garfield County, northeastern Montana, U.S.A., and are based on measurements in Wilson (2004, 2005) and Wilson et al. (in press).

SYSTEMATIC PALEONTOLOGY

LISSAMPHIBIA Haeckel, 1866
CAUDATA Scopoli, 1777
PROTEIDAE Gray, 1825
PARANECTURUS, gen. nov.

Type Species—*Paranecturus garbanii*, sp. nov.

Etymology—From the Greek ‘para’ (beside) and *Necturus* (genus of the caudate family Proteidae), referring to the close phylogenetic relationship.

Diagnosis—As for the type and only species.



FIGURE 1. Maps illustrating provenance of *Paranecturus garbanii*, gen. et sp. nov. **A**, North America with Montana darkened; **B**, state of Montana with Garfield County darkened (modified from Wilson, 2004).

PARANECTURUS GARBANII, sp. nov.
(Figs. 2–6A)

Proteidae gen. et sp. nov.; Wilson et al., in press, fig. 2G, H.

Etymology—Specific epithet after the late Harley J. Garbani for his enormous efforts in collecting and preserving vertebrate fossils from the study area of northeastern Montana, U.S.A.

Holotype—UWBM 93370 (Figs. 2, 3), incomplete atlas missing neural arch roof, crest, and spine, anterior portion of odontoid process, and portions of the anterior and posterior cotylar rims.

Holotype Locality, Age, and Horizon—UWBM C1153 (= UCMP V82022), Garfield County, Montana, U.S.A.; late Maastrichtian, Lancian NALMA; within Hell Creek Formation, ~41.2 m below the Hell Creek–Tullock formational contact.

Referred Specimens—Fragmentary atlantes (n = 27): DMNH 52363, 52367, 55803, 55804, 55814, 56464, 56465, 56466, 56468, 56470; MOR 5375; UCMP 191301, 191538, 556483, 556509, 556586, 556611; UWBM 91059, 91771, 92730, 93364, 93368, 93372, 93377; fragmentary trunk vertebrae (n = 3): MOR 5344; UWBM 94095, 94999.

Referred Specimen Localities, Ages, and Horizons—MOR HC-377, HC-583 (= UCMP V99220); DMNH 3302, 3304, 3305; UCMP V99220 (= MOR HC-583), V99230, V99369; UWBM C1153 (= UCMP V82022); all in Garfield County, Montana, U.S.A.; late Maastrichtian, Lancian NALMA; within lower three-quarters of Hell Creek Formation from ~76.4 to 19.5 m below the Hell Creek–Tullock formational contact.

Diagnosis—Differs from the Sirenidae in having an articular surface of the odontoid process that is not confluent with the anterior cotyles and in lacking transverse processes at the base of the neural arch walls; differs further in having trunk vertebrae lacking the ‘Y’-shaped configuration of the neural crest and paired aliform processes, single-headed rib-bearers on all but the anterior-most trunk vertebrae, anterior basapophyses, and spinal nerve foramina. Differs from the Amphiumidae in lacking a condyle on either side of the ventral midline of the odontoid process of the atlas; differs further in having trunk vertebrae lacking the paired postzygapophyseal crests and anterior basapophyses. Differs from the Batrachosauroididae in having anterior cotyles of atlas that are dorsoventrally compressed and

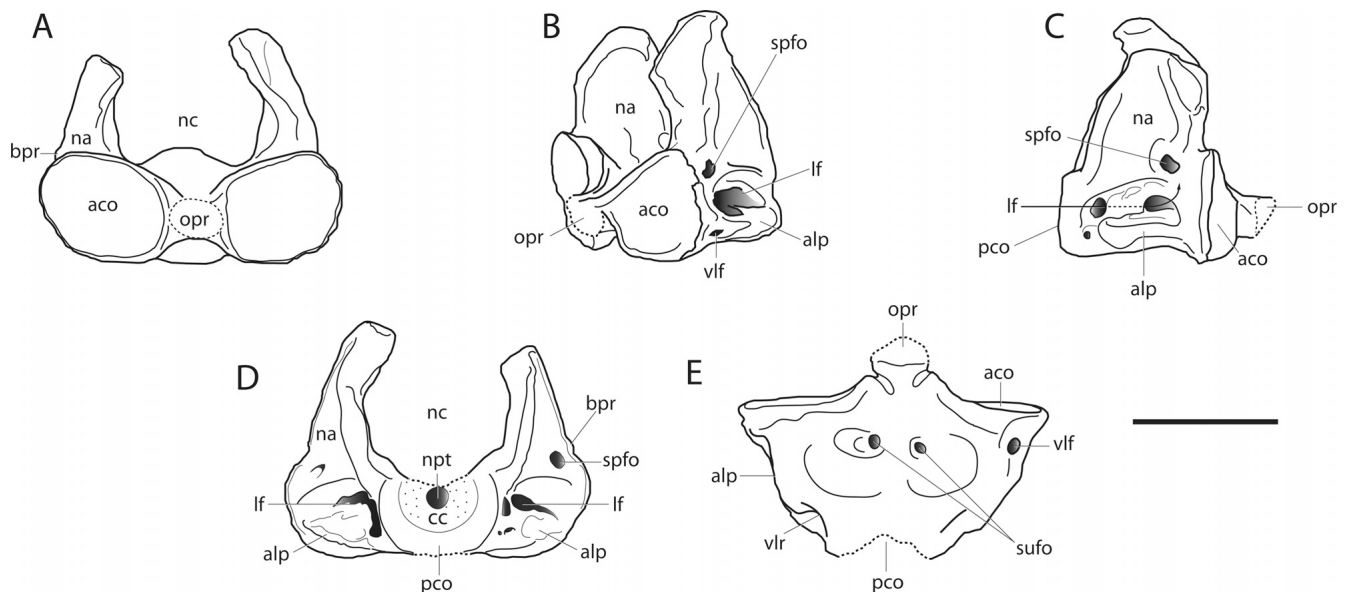


FIGURE 2. Holotype (UWBM 93370) of *Paranecturus garbanii*, gen. et sp. nov., from the Hell Creek Formation, Montana. Labeled line drawings of the atlas in **A**, anterior; **B**, left lateral and anterior; **C**, right lateral; **D**, posterior; and **E**, ventral views. Arrow emphasizes the lateral fossa (lf) by passing behind thin webbing of bone in **C**. Dashed lines represent broken or worn areas. Scale bar equals 1 mm.

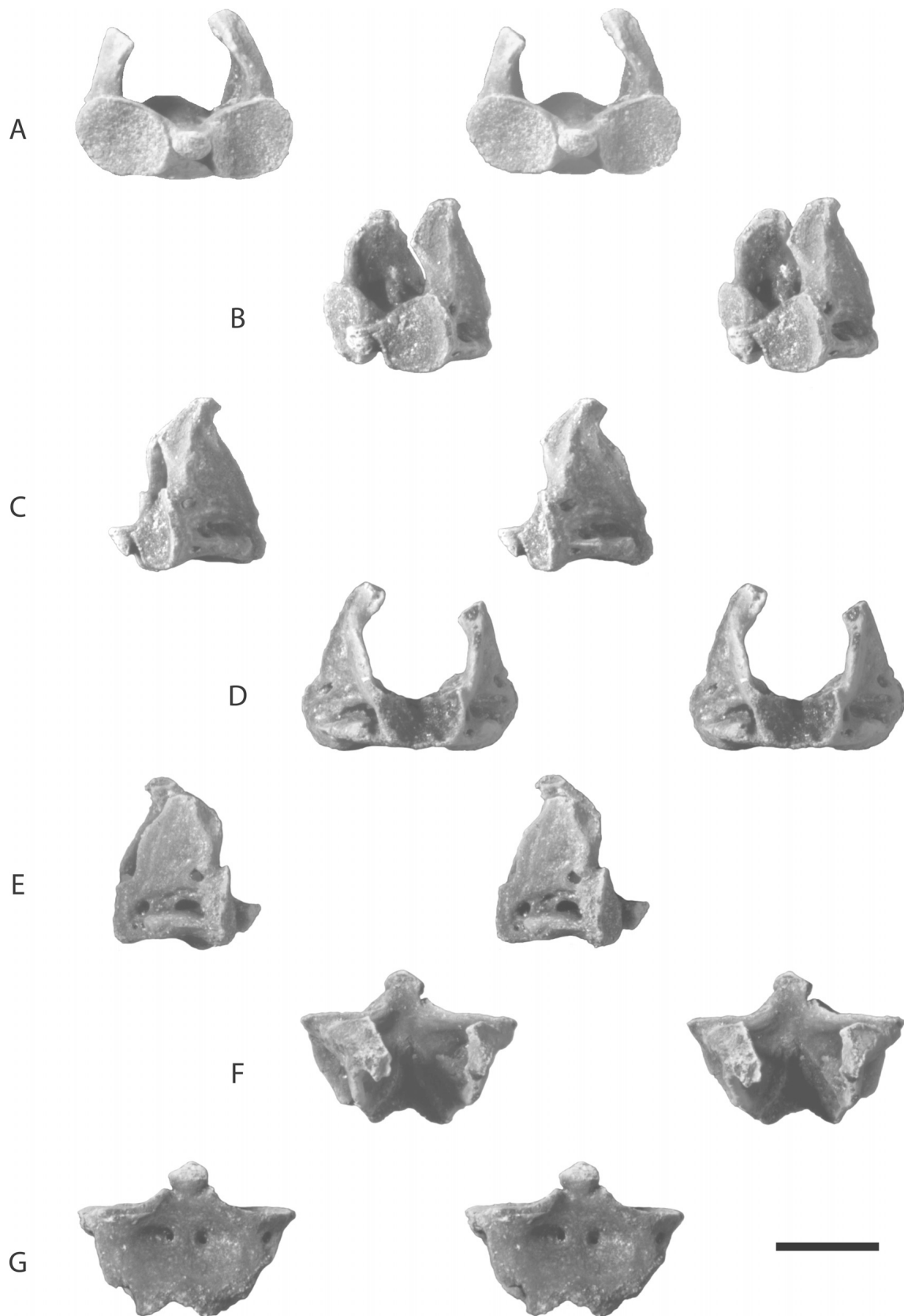


FIGURE 3. Holotype (UWBM 93370) of *Paraneoturus garbanii*, gen. et sp. nov., from the Hell Creek Formation, Montana. Stereophotos of the atlas in **A**, anterior; **B**, left lateral and anterior; **C**, left lateral; **D**, posterior; **E**, right lateral; **F**, dorsal; and **G**, ventral views. Scale bar equals 1 mm.

shallowly concave and in having a prominent odontoid process; differs further in having trunk vertebrae that are amphicoelous (except from *Palaeoproteus*) and in lacking basapophyses (except from *Batrachosauroides* and *Peratosauroides*). Differs from the Scapherpetontidae in having an atlas with an alar-like process along the ventrolateral aspect of centrum; differs further in having trunk vertebrae with a prominent groove on the posterior face of the neural arch and in having solid (i.e., lateral ends not hollow) dorsal rib-bearers. Differs from the proteids *Proteus anguinus*, *Mioproteus caucasicus*, and *Necturus maculosus* in having an articular surface of the odontoid process (atlas unknown for *N. krausei*) not confluent with the anterior cotyles; differs from *P. anguinus* (following atlantal character states uncertain for *M. caucasicus*), but similar to *N. maculosus*, in having an alar-like process along the ventrolateral aspect of centrum; differs from *P. anguinus* and *N. maculosus* in having an odontoid process found at approximately midheight of the anterior cotyles (rather than in the dorsal half), in having neural canal partly between the anterior cotyles (rather than above), and in lacking lateral flanges of the neural arch; differs further from *P. anguinus*, but similar to *N. maculosus*, in having a dorsally concave and perforated ventromedial surface of the centrum (rather than ventrally convex and non-perforated); trunk vertebrae differ from *P. anguinus*, *M. caucasicus*, *N. maculosus*, and *N. krausei* in having generally smaller subcentral foramina; differs from *P. anguinus* and *M. caucasicus*, but similar to *N. maculosus* and *N. krausei*, in having a unicipitate neural spine and divergent, bicipitate rib-bearers; differs from *M. caucasicus*, but similar to *P. anguinus*, *N. maculosus*, and *N. krausei*, in having a short neural crest and in lacking posterior basapophyses; differs further from *N. krausei*, but similar to *N. maculosus*, in having a solid dorsal rib-bearer; differs from *N. maculosus*, but similar to *N. krausei*, in having anteroposteriorly elongate postzygapophyses.

Justification of Association—Association of the atlas and trunk vertebrae of *Paranecturus garbanii* is based on their similar cotylar morphology and size and on co-occurrences within the Hell Creek Formation. The cotyles of the atlas and trunk vertebrae are subcircular to dorsoventrally compressed. They also have a thin layer of calcified cartilage internally and the moderately sized open notochordal pit is slightly above the center. Dimensions of the cotyles are also similar. The width of the posterior cotyle of the holotype (UWBM 93370) is 0.81 mm. The average anterior and posterior cotylar width of the most nearly complete trunk vertebra (UWBM 94999) is 0.85 mm. Similarly, the approximate height of the posterior cotyle of the holotype is 0.72 mm versus an average height of 0.79 mm for the trunk vertebra. Finally, association of the vertebrae is made based on several co-occurrences at the same localities in the Hell Creek Formation. For example, both the holotype (UWBM 93370) and the most nearly complete trunk vertebra (UWBM 94999) come from the same locality (UWBM C1153).

DESCRIPTION

Atlas

Atlantes of *Paranecturus garbanii* (Figs. 2–4) range in intercotylar width from 1.6 to 2.5 mm and in centrum length (including odontoid process) from about 1.1 to 2.0 mm. The average dimensions are 2.0 mm ($n = 23$) and 1.4 mm ($n = 20$), respectively.

The odontoid process (= ‘intercotylar process’ or ‘interglenoid tubercle’ of some authors; e.g., Estes [1981] and Evans and Milner [1993], respectively) of the holotype (UWBM 93370) is damaged anteriorly and is bilaterally asymmetrical (Figs. 2A–C, E, 3A–C, E–G), but resembles referred specimens in most other respects. In the holotype, the process is moderately elongate and set between the medial edges of, and approximately in line with, the dorsoventral midheight of the anterior cotyles. The base of the odontoid process is expanded laterally on the left side, but slightly

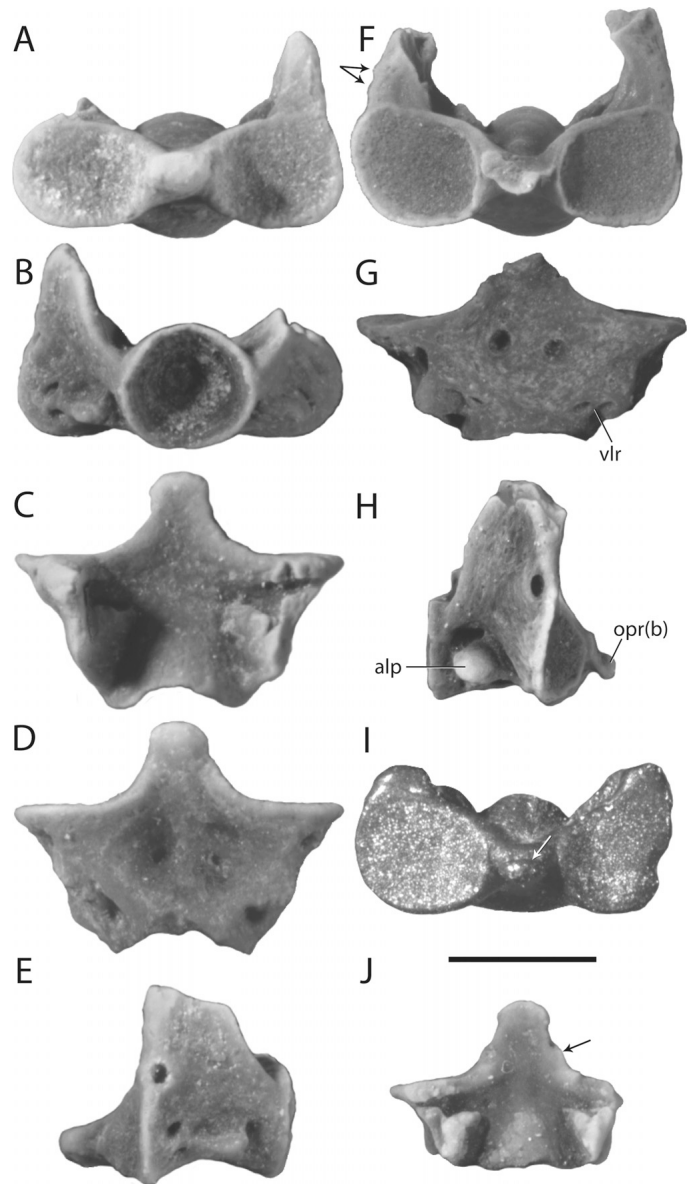


FIGURE 4. Referred atlantes of *Paranecturus garbanii*, gen. et sp. nov., from the Hell Creek Formation, Montana. DMNH 56465 in A, anterior; B, posterior; C, dorsal; D, ventral; and E, left lateral views. UCMP 556611 in F, anterior; G, ventral; and H, right lateral views. I, UCMP 191538 in anterior view. J, UWBM 93372 in dorsal view. Arrows in F and J point to low bony protuberances. See text for explanation of arrows in I and J. Scale bar equals 1 mm.

constricted on the right. In dorsal view, at approximately its midlength, the process becomes restricted before broadening and becoming rounded anteriorly. In lateral view, the odontoid process is thick and extends near the horizontal. Anteriorly, the undamaged portion of the ventral and lateral surfaces is roughened. Specimens preserving a more nearly complete odontoid process indicate that the bilateral asymmetry seen in the holotype is atypical, because all referred specimens have bilaterally symmetrical expanded bases (e.g., DMNH 56465 and UWBM 93372; Fig. 4C and J, respectively). A bilaterally symmetrical odontoid process is the normal condition among caudates.

The anterior cotyles are trapezoidal in anterior outline (Fig. 3A, B). The dorsal cotylar rim is inclined dorsolaterally along

much of its width from the medial aspect of the cotyle and peaks well past the cotylar midwidth. The surface of the anterior cotyles is roughened, slightly concave top to bottom, and moderately concave side to side. Medially, the anterior cotyles are drawn forward onto the base of the odontoid process, and, in lateral view, they taper anteriorly (Fig. 3A–C, E). In dorsal and ventral views, the lateral three-fourths of the anterior cotyles face nearly perpendicular relative to the anteroposterior axis of the centrum (Fig. 3F, G).

The posterior cotyle of the holotype (UWBM 93370) was slightly damaged during examination but shows its original preservation in Figure 3A (see also Fig. 2A). In the undamaged DMNH 56465 (Fig. 4A–E), the posterior cotyle is subcircular, slightly dorsoventrally compressed, lined anteriorly with a thin layer of calcified cartilage, and has a moderately sized open notochordal pit just above its center (Fig. 4B; see also Fig. 2D). In lateral view, the ventral margins of the anterior and posterior cotyles are approximately in line with each other (Fig. 4E).

The centrum of the holotype (UWBM 93370) is short anteroposteriorly and, in dorsal and ventral views, tapers posteriorly. Ventrally, the centrum is concave dorsally and relatively smooth at its center and is perforated by two medial subcentral foramina (Figs. 2E, 3G), one to either side of the midline. A third foramen (Figs. 2B, E, 3C, G) is found posterior to the left anterior cotyle, whereas the right side lacks the same foramen. Along the ventrolateral margin of the centrum there is a moderately thick alar-like process or ridge that projects posteriorly from behind the anterior cotyles (Figs. 2B–E, 3B–G). An anterolaterally arcing ventrolateral ridge (Figs. 2E, 3G) bridges the posterior cotyle and the alar-like process. In lateral view, the centrum is excavated by a lateral fossa (Fig. 2B–D). The lateral fossa is found dorsal to the alar-like process, which, in turn, is bordered medially by a deep groove. The left lateral fossa is open, whereas the right lateral fossa is partially covered roughly at its midlength by a thin webbing of bone that forms an anterior and a posterior opening (Figs. 2B, 3C versus Figs. 2C, 3E; see also Fig. 2D). The right fossa is connected ventromedially to the right subcentral foramen, as evidenced by passing a thin filament through the posterior opening (not figured). Posterior to the right alar-like process are two small openings (Fig. 2C, D). At the same level and position on the opposite side of the centrum the area is non-perforated and open to the left lateral fossa. The ventral margin of the centrum is concave dorsally (Figs. 2C, 3C, E). Immediately behind the anterior cotyle and ventral to the anterior region of the base of the neural arch is an ovoid spinal foramen (Figs. 2B–D, 3B–E). In some specimens, there are small and very low, rounded bony protuberances anterior to the spinal foramen (Fig. 2A and arrows in Fig. 4F).

None of the atlantes possess a complete neural arch. The holotype (UWBM 93370) is the most nearly complete atlas in the sample and it preserves most of the left and right neural arches. In lateral view, the base of the neural arch spans most of the distance between the anterior and posterior cotyles. The anterior margin is directed dorsally and slightly anteriorly and is offset posteriorly from the anterior cotylar rim. In general, the posterior border is sinuous (Figs. 2C, 3C, E). The lateral face of the neural arch wall is shallowly excavated and confluent ventrally with the lateral fossa of the centrum (Figs. 2B–D, 3B–E). The neural arches are widely divergent, forming a broad neural canal (Figs. 2A, D, 3A, D). In anterior view, the lateral edges of the neural arches are inclined at a slight angle medially.

Some notable individual morphological variation exists in the atlantes of *Paranecturus garbanii*. In dorsal view, the relatively complete odontoid process of UWBM 93372 (Fig. 4J) resembles the odontoid process of *Lisserpeton* in being slightly more arrowhead-shaped anteriorly yet maintains the expanded base as in DMNH 56465 (Fig. 4J versus Fig. 4C, respectively). In lateral view, the odontoid process in the holotype (UWBM 93370)

extends approximately horizontally (Fig. 3C, E) versus slightly more ventrally in DMNH 56465 (Fig. 4E). The relatively short and broadly rounded odontoid process of UCMP 191538 is atypical in having a dorsal surface that drops abruptly onto a short shelf-like projection anteriorly (see white arrow in Fig. 4I).

The anterior cotyles of *Paranecturus garbanii* are trapezoidal in outline but can vary in the degree of marginal curvature. For example, the ventral margin can be gently convex (UWBM 93370; Fig. 3A) to broadly rounded (UCMP 191538; Fig. 4I). Likewise, the lateral margin may be roughly straight (DMNH 56465, left anterior cotyle; Fig. 4A), broadly rounded (UCMP 191538; Fig. 4I), or more acutely rounded (UWBM 93370; Fig. 3A), as is the case for the medial margin. The degree of concavity also varies among the anterior cotyles. In dorsal and ventral views of most specimens, the lateral three-fourths or more of the anterior cotyles face nearly perpendicular to the anteroposterior axis of the centrum (e.g., UWBM 93370; Fig. 3F, G), whereas some face slightly more lateroposteriorly at their outermost edges (e.g., UCMP 191538; view not figured). The medial one-fourth or less of the cotyle is drawn forward onto or near the base of the odontoid process (e.g., see black arrow in Fig. 4J) and, in some specimens, this region of the anterior cotyle is oriented nearly perpendicular to the remainder of the cotyle (e.g., UWBM 93370; not figured). A few specimens (e.g., DMNH 55814, 56466; neither figured) have both medial and lateral edges drawn forward forming a posteriorly concave cotylar margin in dorsal view. No major differences in morphology occur in the posterior cotyle.

Ventrally, the centrum bears up to nine medially placed subcentral foramina or pits (Figs. 3G, 4D, G). The alar-like process varies in dorsoventral thickness and length and in some specimens, it is only a round, knob-like protuberance (e.g., DMNH 56465, Fig. 4B, D, E; UCMP 556611, Fig. 4G, H). The lateral fossa may or may not be partially covered by a thin webbing of bone (e.g., UWBM 93370 versus DMNH 56465; Fig. 3B–E versus Fig. 4B, E, respectively). The presence of the ventrolateral foramen can vary among the different atlantes as well as from side to side within the same specimen (e.g., UWBM 93370; Figs. 2E, 3G). The spinal nerve foramen is generally oval in outline, but the outline can vary from being anteroposteriorly to more dorsoventrally compressed (e.g., DMNH 56465 and UWBM 93370, respectively; Fig. 4E versus Fig. 3C, E).

In general, the neural arches of the referred specimens do not vary significantly from the holotype specimen (UWBM 93370). However, in several specimens, the anterior face of the neural arch is flush with the anterior rim of the anterior cotyles (e.g., DMNH 56465 and UCMP 556611; Fig. 4E and H, respectively) versus being offset posteriorly as in the holotype (Figs. 2C, 3C, E). In UCMP 556611, the anterior face of the base of the neural arch is flat and oriented transversely versus anterolaterally as in the holotype.

Trunk Vertebrae

The sample of trunk vertebrae (Fig. 5) includes one nearly complete specimen (UWBM 94999) and two fragmentary specimens (UWBM 94095; MOR 5344). UWBM 94999 (Fig. 5A–H) is missing the anterior portion of the right prezygapophysis, the medial one-half of the left prezygapophysis, and the lateral ends of most of the rib-bearers. UWBM 94095 (Fig. 5I–L) preserves the anterior portion of the centrum and most of the right side including both rib-bearers and the adjacent part of the neural arch. MOR 5344 (Fig. 5M–O) is the posterior half of a centrum.

The vertebra is moderately elongate and low (Fig. 5C, F). UWBM 94999 is 2.8 mm in length and 1.9 mm in height. The centrum is deeply amphicoelous and the cotyles are subcircular (Fig. 5A, D, G, J) to moderately compressed dorsoventrally (Fig. 5M) in outline. In MOR 5344, the dorsal margin of the posterior cotyle is flattened relative to the ventral margin (Fig. 5M). An open and

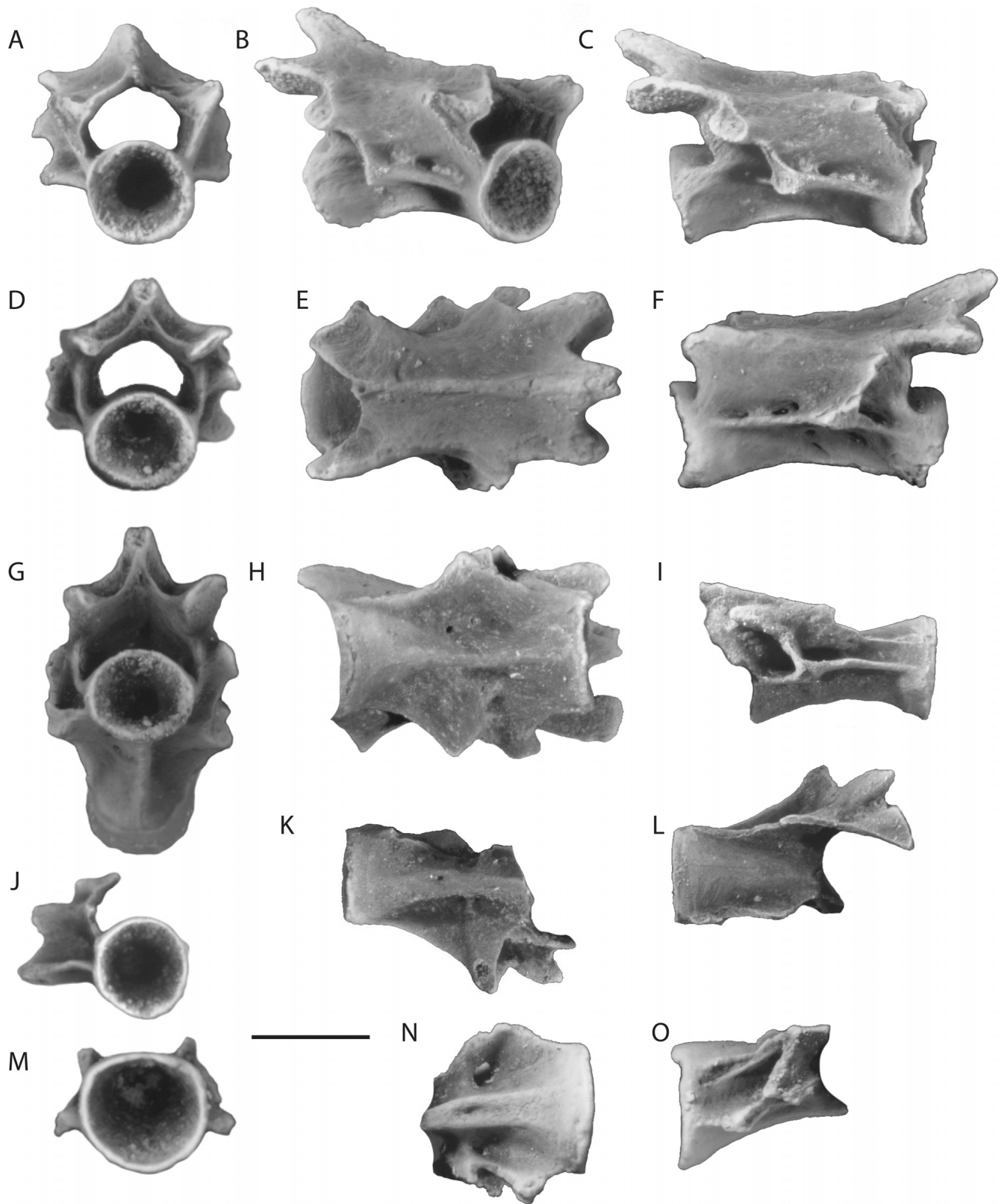


FIGURE 5. Referred trunk vertebrae of *Paraneoturus garbanii*, gen. et sp. nov., from the Hell Creek Formation, Montana. UWBM 94999 in **A**, anterior; **B**, right lateral and anterior; **C**, right lateral; **D**, posterior; **E**, dorsal; **F**, left lateral; **G**, posterior and ventral; and **H**, ventral views. UWBM 94095 in **I**, right lateral; **J**, anterior; **K**, ventral; and **L**, dorsal views. MOR 5344 in **M**, posterior; **N**, ventral; and **O**, right lateral views. Scale bar equals 1 mm.

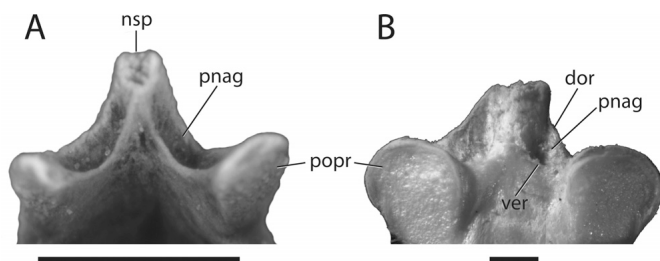


FIGURE 6. Configuration of the groove on the posterior face of the neural arch in **A**, *Paranecturus garbanii*, gen. et sp. nov. (UWBM 94999), and **B**, *Necturus maculosus* (uncatalogued specimen). Scale bars equal 1 mm.

moderately sized notochordal pit is found just above the center of the cotyle. A thin layer of calcified cartilage is present within the cotyles. The subcentral keel is concave dorsally. In ventral view, the subcentral keel varies from being relatively narrow (UWBM 94999; Fig. 5H) to moderately wide (UWBM 94095 and MOR 5344; Fig. 5K and N, respectively). In all three specimens, the anterior and posterior extremities of the keel do not reach the cotylar rims. In UWBM 94095, a small foramen pierces the subcentral keel medially in the anterior half, whereas in MOR 5344 a small foramen pierces the keel in the posterior half (Fig. 5K versus Fig. 5N, respectively). In UWBM 94999, four small subcentral foramina are present: three on the left side and one on the right. The medial-most left foramen is connected to a shallow and narrow groove that is oriented posteroventrally along the side of the subcentral keel (Fig. 5G, H). Two small subcentral foramina are present on the right side of UWBM 94095 (Fig. 5K). One relatively larger posterior subcentral foramen is found on either side of the subcentral keel in MOR 5344 (Fig. 5N). Basapophyses are lacking.

The transverse processes are bicipitate, divergent, and connected by a webbing of bone. Most of the rib-bearers of all three trunk vertebrae are broken laterally except for the left dorsal rib-bearer of UWBM 94999 (Fig. 5F, G), which is only slightly chipped, and the right dorsal rib-bearer of UWBM 94095 (Fig. 5I, L), which is intact. The base of the dorsal rib-bearer arises from the lateral edge of the neural arch roof. The ventral rib-bearer is at roughly the midheight of the centrum. The dorsal rib-bearers are solid (Fig. 5F, I). In UWBM 94999, the left dorsal rib-bearer is short and flattened side to side, whereas in UWBM 94095 the right dorsal rib-bearer is more elongate and oval in cross-section. Because the right dorsal rib-bearer of UWBM 94999 is broken laterally, it cannot be determined if it is solid or hollow. In UWBM 94999, the ventral rib-bearers are relatively larger and both right rib-bearers are more expanded than their left counterparts. The ventral rib-bearer in UWBM 94095 has a small hole at its tip, suggesting that it may have been hollow laterally (Fig. 5K). The alar processes of the ventral rib-bearers are thin and short. The right posterior alar process of UWBM 94999 is restricted to the base of the rib-bearer (Fig. 5H). A narrow vertebralarterial canal passes anteroposteriorly through the base of the transverse process.

The neural canal is vaulted but wider than tall (Fig. 5A, D). The roof of the neural arch is low and essentially flat. In UWBM 94999, a faint anteroposteriorly directed ridge is present along the lateral edge of the neural arch, whereas in UWBM 94095 the ridge is acutely rounded and prominent (Fig. 5B, C, F versus Fig. 5I, J, L). The neural crest is low, narrow, and extends posteriorly from the front of the neural arch to at least the level of the base of the neural spine. The neural spine in UWBM 94999 is unicipitate, low, and extends posteriorly well past the rim of the pos-

terior cotyle. The neural spine is worn posteriorly and along the dorsal crest. The posterior face of the neural arch is indented by a prominent groove to either side of the neural spine (Figs. 5D, G, 6A). The groove is bounded dorsally and ventrally by a ridge (Fig. 6A). The ventral ridge is lamellar and forms an acutely 'V'-shaped flange directly beneath the neural spine. No spinal foramina pierce the neural arch walls.

The preserved portions of the prezygapophyses indicate that they likely were oval in outline (Fig. 5E). The prezygapophyseal facets are tipped dorsally and medially at their lateral edges. The postzygapophyses are anteroposteriorly elongate and the facets are elliptical in outline (Fig. 5C, F, H). In UWBM 94999, the right postzygapophysis is larger and more rectangular in dorsal outline than the left (Fig. 5E). In posterior view, the postzygapophyses are inclined laterally at $\sim 35^\circ$ from the horizontal (Fig. 5D). In lateral view, the left and right postzygapophyses range in posterior inclination from $\sim 4^\circ$ to $\sim 12.5^\circ$ from the horizontal, respectively. In UWBM 94999, the anterolateral margin of the postzygapophysis is nearly confluent with the base of the dorsal rib-bearer.

Remarks—Based on the unique combination of vertebral character states described above, it is apparent that *Paranecturus garbanii*, gen. et sp. nov., is a distinct caudate. *P. garbanii* possesses a suite of vertebral character states allying it with *Necturus*, *Proteus*, and *Mioproteus* (atlas with dorsoventrally compressed anterior cotyles, trunk vertebrae deeply amphicoelous with little calcified cartilage lining the cotylar walls, subcircular cotyles, low neural spine, and lack of spinal nerve foramina), with *Necturus* and *Proteus* (atlas with prominent odontoid process, trunk vertebrae with low neural crest, presence of a groove on the posterior face of the neural arch, and lack of basapophyses), and, more exclusively, with *Necturus* (atlas with shallowly concave anterior cotyles, presence of alar-like process of centrum, trunk vertebrae with unicipitate neural spines, divergent rib-bearers, and solid dorsal rib-bearers). Together, these features support assigning *P. garbanii* to the Proteidae. However, there are considerable differences in atlantal morphology between *Paranecturus*, *Necturus*, and *Proteus* (the following atlantal character states are uncertain for *Mioproteus*), such as the lack of a confluent articular surface between the odontoid process and the anterior cotyles, the odontoid process set at midheight of the anterior cotyles (rather than in the upper half), and the neural arch partly between the anterior cotyles (rather than above). These character states, in addition to having dorsoventrally compressed and shallowly concave anterior cotyles, are also seen in the Scapherpetontidae (e.g., *Scapherpeton*, *Lisserpeton*), which raises the possibility that *P. garbanii* represents a small scapherpetontid. Nevertheless, the presence and configuration of the alar-like process along the ventrolateral margin of the centrum is inconsistent with known scapherpetontids. In contrast, it shares this feature with some atlantes (three out of five examined) of *N. maculosus* and with some batrachosauroids, which are thought to be closely related to proteids (e.g., Naylor, 1978b, 1979; Estes, 1981). Both *Opisthotriton kayi* and *Prodesmodon copei* have an alar-like process showing varying degrees of development (e.g., Estes, 1964:figs. 38F and 42C, respectively; see also Estes, 1975:fig. 2C, D; Gardner, 2000).

Many features of the trunk vertebrae of *Paranecturus garbanii* are also shared among scapherpetontids (amphicoelous centra, unicipitate neural spines, divergent rib-bearers of the transverse process, and lack of basapophyses and spinal nerve foramina). However, the presence of a well-developed groove on the posterior face of the neural arch is lacking in specimens of *Scapherpeton* and *Lisserpeton* available to me and in the two species of *Piceoerpeton* based on figured and described specimens in the literature (e.g., Estes, 1981; Naylor and Krause, 1981; Gardner, 2012). This feature is prominent in *N. maculosus* (Fig. 6B; see also Naylor, 1978a:fig. 2), in the holotype of *N. krausei* (UALVP 14310; Naylor, 1978a:fig. 1A), and to a lesser extent, in *Proteus anguinus* (pers. observ.). In addition, the solid dorsal rib-bearer

TABLE 1. List of caudates used for the phylogenetic analyses and their temporal and biogeographic ranges.

Taxon	Age	Biogeography	References
<i>Cryptobranchus alleganiensis</i>	late Pleistocene–Recent	eastern U.S.A.	11
<i>Necturus maculosus</i>	late Pleistocene–Recent	southeastern Canada and eastern U.S.A.	11
<i>Proteus anguinus</i>	Recent	southeastern Europe	16
<i>Opisthotriton kayi</i>	Santonian–late Paleocene	western Interior of Canada and U.S.A.	5, 6, 10
<i>Prodesmodon copei</i>	late Campanian–early Paleocene	western Interior of Canada and U.S.A.	1, 2, 5, 6, 10, 19
<i>Scapherpeton tectum</i>	Santonian–late Paleocene	western Interior of Canada and U.S.A.	2, 5, 6, 10
<i>Lisserpeton bairdi</i>	late Campanian–middle Paleocene	western Interior of Canada and U.S.A.	1, 3, 5, 6, 10
<i>Piceoerpeton willwoodense</i>	late Paleocene–early Eocene	western Interior of Canada and U.S.A.; Ellesmere Island, Canada	5, 9, 15
<i>Piceoerpeton naylori</i>	late Maastrichtian–?early Paleocene	Montana and Wyoming, U.S.A.	9, 12, 17
<i>Proamphiuma cretacea</i>	?late Maastrichtian–early Paleocene	Montana, U.S.A.	4, 5, 7, 17
<i>Habrosaurus dilatus</i>	late Maastrichtian–middle Paleocene	western Interior of Canada and U.S.A.	2, 5, 8
<i>Necturus krausei</i>	late Paleocene	Saskatchewan, Canada	5, 13, 14
<i>Paranecturus garbanii</i>	late Maastrichtian	Montana, U.S.A.	17, 18

References: 1, DeMar and Breithaupt (2006); 2, Estes (1964); 3, Estes (1965); 4, Estes (1969); 5, Estes (1981); 6, Gardner (2000); 7, Gardner (2003a); 8, Gardner (2003b); 9, Gardner (2012); 10, Gardner et al. (in press); 11, Holman (2006); 12, Naylor (1983); 13, Naylor (1978a); 14, Naylor (1978b); 15, Naylor and Krause (1981); 16, Sket (1997); 17, Wilson et al. (in press); 18, this paper; 19, personal observation.

seen in the trunk vertebrae of *P. garbanii* is also found in some vertebrae of *N. maculosus*, but not in any known scapherpetontid.

PHYLOGENETIC ANALYSIS

Methods

I conducted a series of phylogenetic analyses in order to explore relationships of the new taxon among select caudates. The first set of analyses was conducted using TNT version 1.1 (Goloboff et al., 2008). The data matrix was created using Mesquite version 2.75 (Maddison and Maddison, 2011). The matrix includes 13 taxa and 23 characters from the atlas and trunk vertebrae. The character matrix created by Denton and O'Neill (1998) and later revised by Gardner (2000) formed the basis of the analyses. Minor modifications and additions were made (list of characters, Appendix 1; character matrix, Appendix 2). All characters were unordered and were equally weighted. The first phylogenetic analysis includes all 13 taxa, whereas the second analysis excludes the fossil proteid *Necturus krausei*, because more than half (57%) of the characters of *N. krausei* are not scorable (see Appendix 2). The extant cryptobranchid *Cryptobranchus alleganiensis* was chosen as the outgroup, because cryptobranchoids are widely considered to occupy a basal position among crown-group salamanders or Urodela (e.g., Gao and Shubin, 2001; Roelants et al., 2007) and was used to polarize character states. The ingroup includes mostly Late Cretaceous to early Eocene caudates from the Western Interior of Canada and the U.S.A. Two extant and one late Paleocene proteid were also included. Members of the ingroup were chosen specifically to test the proteid versus scapherpetontid affinities of *P. garbanii*. The ingroup comprises the amphiumid *Proamphiuma cretacea*; the batrachosauroidids *Opisthotriton kayi* and *Prodesmodon copei*; the proteids *N. krausei*, *N. maculosus*, and *Proteus anguinus*; the scapherpetontids *Scapherpeton tectum*, *Lisserpeton bairdi*, *Piceoerpeton willwoodense*, and *P. naylori*; the sirenid *Habrosaurus dilatus*; and the new taxon, *Paranecturus garbanii* (see Table 1 for the ages and biogeographic ranges of each taxon). Exhaustive searches (implicit enumeration) were performed to find the most parsimonious trees. Bremer and bootstrap values are reported. Bootstrap values are based on 10,000 replicates. The last set of phylogenetic analyses is based on the results (i.e., most parsimonious tree topology) from the second exhaustive search excluding *N. krausei*. I performed a heuristic search in PAUP* version 4.0b10 (Swofford, 2002) of two alternative topologies to determine the difference in tree length between the single most parsimonious tree and one in which monophyly was enforced between *P. garbanii* and the Scapherpetontidae.

monious tree and one in which monophyly was enforced between *P. garbanii* and the Scapherpetontidae.

Results

The first set of phylogenetic analyses using the exhaustive search method recovered similar topologies regardless of whether or not *Necturus krausei* was included (Fig. 7A versus Fig. 7B). Inclusion of *N. krausei* resulted in three most parsimonious trees (strict consensus shown in Fig. 7A; tree length = 49 steps; consistency index [CI] = 0.633; retention index [RI] = 0.640), whereas only one most parsimonious tree (Fig. 7B; tree length = 49 steps; CI = 0.633; RI = 0.640) was recovered when *N. krausei* was excluded from the analysis. Both exhaustive searches recovered a monophyletic Batrachosauroididae (*Opisthotriton kayi* + *Prodesmodon copei*; Fig. 7A, B, Node B) and Scapherpetontidae ((*Piceoerpeton willwoodense* + *P. naylori*) + (*Scapherpeton tectum* + *Lisserpeton bairdi*); Fig. 7A, B, Node S) and a sister-pair relationship between the amphiumid *Proamphiuma cretacea* and the sirenid *Habrosaurus dilatus* (Fig. 7A, B). The strict consensus including *N. krausei* places *Paranecturus garbanii* in an unresolved polytomy with the proteids *N. krausei*, *N. maculosus*, and *Proteus anguinus* (Fig. 7A, Node P). Exclusion of *N. krausei* resulted in *P. garbanii* being the sister taxon to the extant proteids (Fig. 7B, Node P). Both exhaustive searches recovered similar Bremer and bootstrap values (see values above and below branches, respectively, leading to the nodes in Fig. 7A, B). The batrachosauroidids, scapherpetontids, and the genus *Piceoerpeton* are moderately supported (i.e., decay index = 2; bootstrap $\geq 50\%$), whereas all other nodes are weakly supported (i.e., decay index = 1; bootstrap $< 50\%$). Results from the heuristic search indicate that removal of *P. garbanii* from the Proteidae (i.e., from the most parsimonious tree topology) and enforcing strict monophyly of *P. garbanii* with the Scapherpetontidae requires one additional step (tree length = 50 versus 51 steps, respectively).

Remarks—The phylogenetic relationships presented here are based on atlantal and trunk vertebral character states only, and thus, the higher-level relationships of the ingroup (i.e., Amphiumidae, Batrachosauroididae, Proteidae, Scapherpetontidae, Sirenidae) are tentative. Previous work based on qualitative assessments and on more nearly complete specimens or suites of elements than those used here suggested a sister-taxon relationship between the Batrachosauroididae and Proteidae (Estes, 1975, 1981; Estes and Darevsky, 1978; Naylor, 1978a, 1978b, 1979,

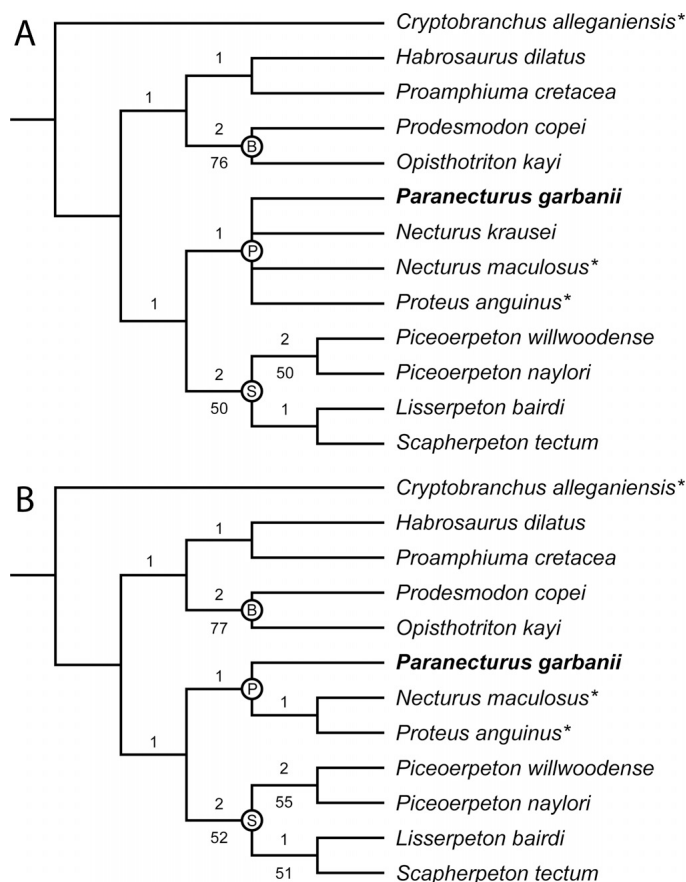


FIGURE 7. Phylogenetic hypotheses resulting from parsimony analysis. **A**, strict consensus of three most parsimonious trees (49 steps; consistency index [CI] = 0.633; retention index [RI] = 0.640) including all 13 taxa based on an exhaustive search; **B**, single most parsimonious tree (49 steps; CI = 0.633; RI = 0.640) excluding *Necturus krausei* based on an exhaustive search. Node B = Batrachosauroididae, Node P = Proteidae, and Node S = Scapherpetontidae. Asterisks (*) indicate extant taxa. Values above branches leading to the nodes represent Bremer support, whereas the values below the branches are the bootstrap values $\geq 50\%$.

1981). More complete sampling of taxa and characters might help resolve the higher-level relationships of these taxa.

DISCUSSION AND CONCLUSIONS

Several character states observed in *Paranecturus garbanii*, gen. et sp. nov., provide evidence for assigning it to the Proteidae. Among these are characters states that are most notably present in *Necturus maculosus*, such as the alar-like process of the atlas (character 10, state 1) and the solid dorsal rib-bearers (character 21, state 1) and neural arch groove (character 23, state 1) of the trunk vertebrae. In addition, the results of the phylogenetic analysis provide a testable hypothesis for the affinities of *P. garbanii* and indicate that *P. garbanii* is likely a basal proteid (Fig. 7A, B).

Paranecturus garbanii represents a latest Cretaceous proteid. Reports of pre-Cenozoic proteids such as the Late Jurassic *Comonecturoides* (Hecht and Estes, 1960) and the Early Cretaceous *Hylaeobatrachus croyi* (Dollo, 1884; Herre, 1935) are better regarded as Caudata incertae sedis (Estes, 1981). Owing to its relationship with the late Paleocene *Necturus krausei*, the presence of *P. garbanii* in the latest Cretaceous implies that the lineage survived the Cretaceous-Paleogene mass extinction. This hypothesis is consistent with molecular divergence esti-

mates, which also support a pre-Cenozoic origin for the Proteidae (e.g., Roelants et al., 2007; Zhang and Wake, 2009).

The fossil record of proteids is still poor (Naylor, 1978a; Estes, 1981). Thus, the discovery of the fossil proteid *Paranecturus garbanii* adds significantly to our understanding of the clade's evolution. Based on specimens of *P. garbanii*, it can be postulated when certain character states of the atlas and trunk vertebrae evolved in this lineage. For example, the lateral flanges of the atlas (character 11) had not yet evolved in the Proteidae by the end of the Cretaceous, whereas the alar-like process (character 10) seen in *Necturus* had. Discovery of atlantes of *Necturus krausei* may aid in determining more precisely when certain other atlantal features evolved in the *Necturus* lineage.

ACKNOWLEDGMENTS

I thank G. P. Wilson, C. Sidor, L. Tsuji, S. Nesbitt, J. Calede, J. Grummer (University of Washington, Seattle, Washington [UW]), and J. Gardner (Royal Tyrrell Museum of Palaeontology, Drumheller, Alberta) for helpful reviews, discussions, or technical support, on topics related to this project. Additional thanks to J. Gardner for providing relevant literature and SEM images of *Necturus krausei* for comparison. A. Leaché, K. Petersen (UW), and D. Wake (University of California, Berkeley, California) provided access to skeletonized specimens of *Cryptobranchus alleganiensis*, *Necturus maculosus*, and *Proteus anguinus*, respectively. Reviews by J. Gardner and P. Skutschas (Saint Petersburg State University, Saint Petersburg, Russia) and editorial comments by J. Anderson (University of Calgary, Alberta, Canada) were valuable in improving the manuscript. The Bureau of Land Management, Charles M. Russell Wildlife Refuge, and Montana Fish, Wildlife, and Parks have provided logistical support and special use permits for the collection of the vertebrate fossils studied here. This material, in part, is based upon work supported by the National Science Foundation Graduate Research Fellowship under grant DGE-0718124.

LITERATURE CITED

- Abramoff, M. D., P. J. Magalhaes, and S. J. Ram. 2004. Image Processing with ImageJ. *Biophotonics International* 11:36–42.
- Bryant, L. J. 1989. Non-dinosaurian lower vertebrates across the Cretaceous-Tertiary boundary in northeastern Montana. *University of California Publications in Geological Sciences* 134:1–107.
- DeMar, D. G., Jr. 2011. New taxonomic, paleobiogeographic, and biostratigraphic records of fossil salamanders (Caudata) from the Hell Creek and Tullock formations of Garfield County, Montana. *Journal of Vertebrate Paleontology* 31(Program and Abstracts 2011):98A.
- DeMar, D. G., Jr., and B. Breithaupt. 2006. The nonmammalian vertebrate microfossil assemblages of the Mesaverde Formation (Upper Cretaceous, Campanian) of the Wind River and Bighorn basins, Wyoming; pp. 33–54 in S. G. Lucas and R. M. Sullivan (eds.), *Late Cretaceous Vertebrates from the Western Interior*. New Mexico Museum of Natural History and Science Bulletin 35.
- Denton, R. K., Jr., and R. C. O'Neill. 1998. *Parrisia neocesariensis*, a new batrachosauroidid salamander and other amphibians from the Campanian of eastern North America. *Journal of Vertebrate Paleontology* 18:484–494.
- Dollo, L. 1884. Note sur le Batracien de Bernissart. *Bulletin du Musée Royal d'Histoire Naturelle de Belgique* 3:85–93.
- Estes, R. 1964. Fossil vertebrates from the Late Cretaceous Lance Formation of eastern Wyoming. *University of California Publications in Geological Sciences* 49:1–187.
- Estes, R. 1965. A new fossil salamander from Montana and Wyoming. *Copeia* 1965:90–95.
- Estes, R. 1969. The fossil record of amphiumid salamanders. *Breviora* 322:1–11.
- Estes, R. 1975. Lower vertebrates from the Fort Union Formation, late Paleocene, Big Horn Basin, Wyoming. *Herpetologica* 31:365–385.
- Estes, R. 1981. Gymnophiona, Caudata. *Encyclopedia of Paleoherpétology*, Part 2. Gustav Fischer Verlag, Stuttgart, 115 pp.

- Estes, R., and P. Berberian. 1970. Paleoeology of a Late Cretaceous vertebrate community from Montana. *Breviora* 343:1–35.
- Estes, R., and I. Darevsky. 1977. Fossil amphibians from the Miocene of the North Caucasus, U.S.S.R. *Journal of the Palaeontological Society of India* 20:164–169.
- Evans, S. E., and A. R. Milner. 1993. Frogs and salamanders from the Upper Jurassic Morrison Formation (Quarry Nine, Como Bluff) of North America. *Journal of Vertebrate Paleontology* 13: 24–30.
- Gao, K.-Q., and N. H. Shubin. 2001. Late Jurassic salamanders from northern China. *Nature* 410:574–577.
- Gardner, J. D. 2000. Systematics of albanerpetontids and other lissamphibians from the Late Cretaceous of western North America. Ph.D. dissertation, University of Alberta, Edmonton, Alberta, 577 pp.
- Gardner, J. D. 2003a. The fossil salamander *Proamphiuma cretacea* Estes (Caudata: Amphiumidae) and relationships within the Amphiumidae. *Journal of Vertebrate Paleontology* 23:769–782.
- Gardner, J. D. 2003b. Revision of *Habrosaurus* Gilmore (Caudata; Sirenidae) and relationships among sirenid salamanders. *Palaeontology* 46:1089–1122.
- Gardner, J. D. 2005. Lissamphibians; pp. 186–199 in P. J. Currie and E. B. Koppelhus (eds.), *Dinosaur Provincial Park: A Spectacular Ancient Ecosystem Revealed*. Indiana University Press, Bloomington, Indiana.
- Gardner, J. D. 2012. Revision of *Piceoerpeton* Meszöely (Caudata: Scapherpetontidae) and description of a new species from the late Maastrichtian and ?early Paleocene of western North America. *Bulletin de la Société Géologique de France* 183:611–620.
- Gardner, J. D., J. G. Eaton, and R. L. Cifelli. In press. Preliminary report on salamanders (Lissamphibia; Caudata) from the Late Cretaceous (late Cenomanian–late Campanian) of southern Utah, U.S.A.; in A. L. Titus and M. A. Lowen (eds.), *At the Top of the Grand Staircase: The Late Cretaceous of Southern Utah*. Indiana University Press, Bloomington, Indiana.
- Goloboff, P. A., J. S. Farris, and K. C. Nixon. 2008. TNT, a free program for phylogenetic analysis. *Cladistics* 24:774–786.
- Gray, J. E. 1825. A synopsis of the genera of reptiles and Amphibia, with a description of some new species. *Annals of Philosophy (Series 2)* 10:193–217.
- Haeckel, E. 1866. *Generelle Morphologie der Organismen* (two volumes). Reimer, Berlin, 574 pp. (Volume 1), 461 pp. (Volume 2).
- Hecht, M. K., and R. Estes. 1960. Fossil amphibians from Quarry Nine. *Postilla* 46:1–19.
- Herre, W. 1935. Die Schwanzlurche der mitteleocänen (oberlutetischen) Braunkohle des Geiseltales und der Phylogenie der Urodelen unter Einschluss der fossilen Formen. *Zoologica (Stuttgart)* 33:1–85.
- Holman, J. A. 2006. Fossil Salamanders of North America. Indiana University Press, Bloomington, Indiana, 232 pp.
- Maddison, W. P., and D. R. Maddison. 2011. Mesquite: A Modular System for Evolutionary Analysis, version 2.75. Available at <http://mesquiteproject.org>. Accessed December 5, 2011.
- Naylor, B. G. 1978a. The earliest known *Necturus* (Amphibia, Urodela), from the Paleocene Ravenscrag Formation of Saskatchewan. *Journal of Herpetology* 12:565–569.
- Naylor, B. G. 1978b. The systematics of fossil and recent salamanders (Amphibia: Caudata), with special reference to the vertebral column and trunk musculature. Ph.D. dissertation, University of Alberta, Edmonton, Alberta, 857 pp.
- Naylor, B. G. 1979. The Cretaceous salamander *Prodesmodon* (Amphibia: Caudata). *Herpetologica* 35:11–20.
- Naylor, B. G. 1981. A new salamander of the family Batrachosauroididae from the late Miocene of North America, with notes on other batrachosauroidids. *PaleoBios* 39:1–14.
- Naylor, B. G. 1983. New salamander (Amphibia: Caudata) atlantes from the Upper Cretaceous of North America. *Journal of Paleontology* 57:48–52.
- Naylor, B. G., and D. W. Krause. 1981. *Piceoerpeton*, a giant Early Tertiary salamander from western North America. *Journal of Paleontology* 55:507–523.
- Roelants, K., D. J. Gower, M. Wilkinson, S. P. Loader, S. D. Biju, K. Guillaume, L. Moriau, and F. Bossuyt. 2007. Global patterns of diversification in the history of modern amphibians. *Proceedings of the National Academy of Sciences of the United States of America* 104:887–892.
- Scopoli, G. A. 1777. *Introductio ad Historiam Naturalem*. Wolfgang Gerle, Prague, 506 pp.
- Sket, B. 1997. Distribution of *Proteus* (Amphibia: Urodela: Proteidae) and its possible explanation. *Journal of Biogeography* 24:263–280.
- Swofford, D. L. 2002. PAUP*. *Phylogenetic Analysis Using Parsimony (*And Other Methods)*, version 4. Sinauer Associates, Sunderland, Massachusetts.
- Wilson, G. P. 2004. A quantitative assessment of mammalian change leading up to and across the Cretaceous-Tertiary boundary in northeastern Montana. Ph.D. dissertation, University of California, Berkeley, California, 412 pp.
- Wilson, G. P. 2005. Mammalian faunal dynamics during the last 1.8 million years of the Cretaceous in Garfield County, Montana. *Journal of Mammalian Evolution* 12:53–75.
- Wilson, G. P., D. G. DeMar Jr., and G. Carter. In press. Extinction and survival of salamander and salamander-like amphibians across the Cretaceous-Paleogene boundary in northeastern Montana, U.S.A.; in G. P. Wilson, W. A. Clemens, J. R. Horner, and J. Hartman, *Through the End of the Cretaceous in the Type Locality of the Hell Creek Formation in Montana and Adjacent Areas*. Geological Society of America Special Paper.
- Zhang, P., and D. B. Wake. 2009. Higher-level salamander relationships and divergence dates inferred from complete mitochondrial genomes. *Molecular Phylogenetics and Evolution* 53:492–508.

Submitted April 7, 2012; revisions received September 20, 2012;

accepted September 25, 2012.

Handling editor: Jason Anderson.

APPENDIX 1. Description of characters used in the phylogenetic analyses. Some character descriptions are modified from previous studies and those are formatted as: (author:character number). **Abbreviations:** DO, Denton and O'Neill (1998); G, Gardner (2000). Additional characters are polarized with respect to *Cryptobranchus alleganiensis*.

Atlas

- (1) Relative depth of anterior cotyles: nearly flat to shallowly excavated (0); moderate to deeply excavated (1) (DO:6; G:4).
- (2) Outline of anterior cotyles: subcircular (0); compressed dorsoventrally (1); compressed lateromedially (2) (DO:4; G:5).
- (3) Form of odontoid process: anteriorly elongate knob (0); dorsoventrally flattened and reduced in length (1); dorsoventrally flattened and reduced further to a horizontal bar (2) (DO:7; G:6).
- (4) Position of neural canal relative to anterior cotyles: above (0); partly between (1) (G:7).
- (5) Dorsal outline of posterior margin of neural arch roof: truncate or pointed (0); forked (1) (DO:8; G:10).
- (6) Dorsal outline of neural crest: broadens posteriorly (0); narrows posteriorly (1) (DO:9; G:11).
- (7) Condition of anterior end of neural crest in dorsal view: not emarginated laterally (0); emarginated laterally (1) (G:12).
- (8) Postzygapophyses: prominent and laterally divergent (0); smaller and directed more ventrolaterally (1); "... weakly developed and does not project ventrally or laterally any significant distance from the neural arch" (2; Gardner, 2003a:774) (DO:10; G:13).
- (9) Condition of articular surface of odontoid process: large (0); small (1); absent (2) (this paper).
- (10) Alar-like process of centrum: absent (0); present (1) (this paper).
- (11) Lateral flanges of neural arch: absent (0); present (1) (this paper).
- (12) Condition of articular surface of odontoid process and anterior cotyles: not confluent (0); confluent (1) (this paper).

- (13) Position of odontoid process relative to anterior cotyles: midheight or lower (0); upper one-half (1) (this paper).

Trunk Vertebrae

- (14) Form of centrum: amphicoelous (0); semi-opisthocoelous (1); fully opisthocoelous (2) (DO:11; G:16).
- (15) Posterior basapophyses: absent (0); present (1) (DO:13, 14; G:17).
- (16) Anterior basapophyses: absent (0); present (1) (DO:13, 14).
- (17) Position of ventral margin of subcentral keel in lateral view of middle trunk vertebrae relative to ventral margin of anterior and posterior cotyles: above (0); approximately in line (1); below (2) (this paper).
- (18) Height of neural spine: low (0); high (1) (DO:16; G:18).
- (19) Height of neural crest of middle trunk vertebrae: low, gently rises posteriorly onto base of neural spine (0); moderate in height, rises at a more pronounced angle posteriorly relative to dorsal surface of neural arch roof (1); high, rises at a pronounced angle and is equal to or greater than the height of the neural spine (2) (this paper).
- (20) Form of transverse process: bicipitate and appressed (0); bicipitate and divergent (1); unicipitate (2) (DO:17; G:19).
- (21) Form of transverse process and condition of lateral ends of rib-bearer(s) of middle trunk vertebrae: bicipitate with dorsal and ventral rib-bearers hollow (0); bicipitate with dorsal rib-bearer solid and ventral rib-bearer hollow (1); unicipitate and solid (2) (this paper).
- (22) Condition of neural spine: finished in cartilage (0); finished in bone (1) (DO:19; G:20).
- (23) Mediolateral groove on the posterior face of the neural arch spanning between the neural spine and postzygapophyses: absent (0); present (1) (this paper).

APPENDIX 2. Character-taxon matrix used for phylogenetic analysis. Polymorphic states are identified as: **A** (0, 1); **B** (1, 2).

	10	20	23
<i>Cryptobranchus alleganiensis</i>	0000000000	0000000000	000
<i>Proteus anguinus</i>	0100110000	1110001002	201
<i>Necturus maculosus</i>	010000000A	1110000001	A01
<i>Necturus krausei</i>	-----	---0000001	001
<i>Paranecturus garbanii</i>	0101----01	0000000001	1-1
<i>Opisthotriton kayi</i>	10B1A101BA	0001102000	010
<i>Prodesmodon copei</i>	1221010121	0002102002	210
<i>Scapherpeton tectum</i>	0101101000	0000002111	000
<i>Lisserpeton bairdi</i>	0101011000	0000001111	000
<i>Piceoerpeton willwoodense</i>	1111-00020	0000001111	000
<i>Piceoerpeton naylori</i>	1111----20	0000000-11	0-0
<i>Habrosaurus dilatatus</i>	0100---00	0100010022	210
<i>Proamphiuma cretacea</i>	1001010200	0000010022	210